SUPEREXCHANGE AND ELECTRON TRANSFER IN THE PHOTOSYNTHETIC REACTION CENTER

Yuming HU and Shaul MUKAMEL [1]
Chemistry Department, University of Rochester, Rochester, NY 14627, USA

Received 22 May 1989

The relative magnitude of the sequential and superexchange electron transfer mechanisms in the primary electron transfer event in a reaction center is a controversial issue. One complication in resolving this problem is that the conventional superexchange theory is valid only when the intermediate energy level is sufficiently high. The precise position of this level in the reaction center is not known, and it is not clear whether this condition is met. We present a novel expression for the superexchange rate in a three-level system, which holds for arbitrary values of the system free energies and reorganization energies. Implications as to the relative contribution of the superexchange and sequential mechanisms are discussed.

1. Introduction

The mechanism for fast electron transfer in reaction centers is one of the many interesting puzzles in understanding the primary events in photosynthesis [1,2]. In the photosynthetic reaction center an electron moves in 2.8 ps over a distance of 17 Å from a bacteriochlorophyll dimer (P) to bacteriopheophytin (H) via an intermediate bacteriochlorophyll monomer (B). The model system suggested for the electron transfer in the reaction center (RC) [3,4] involves three electronic configurations. Using the notation of Marcus, we denote these states (P^*BH, P^+B^-H and P^+BH^-) as $|1\rangle$, $|2\rangle$, and $|3\rangle$, respectively. State $|1\rangle$ is the optically excited chlorophyll dimer state, state $|3\rangle$ is the charge transfer state observed after 2.8 ps and state $|2\rangle$ is a possible intermediate state. The complete kinetic scheme for this system involves a 3×3 rate matrix whose matrix elements K_{jn} denotes the transition rate from state $|n\rangle$ to state $|j\rangle$; $n, j=1, 2, 3$. Since a direct (through space) coupling between states $|1\rangle$ and $|3\rangle$ is excluded by the large separation of P and H, there are two basic mechanisms that have been suggested for the electron transfer process [3,4]. The first is superexchange, whereby $|2\rangle$ serves as an intermediate virtual state. When level $|2\rangle$ is sufficiently higher in energy than $|1\rangle$ and $|3\rangle$ the superexchange rate is given by

$$K_{31} = \frac{2\pi}{\hbar} |V_{SE}|^2 S . \tag{1}$$

Here S is a Franck–Condon-weighted density of states and V_{SE} is the superexchange coupling,

$$V_{SE} = \frac{V_{12} V_{23}}{\Delta G^0_{12} - \lambda_{12}} . \tag{2}$$

ΔG^0_{12} is the free energy difference between states $|1\rangle$ and $|2\rangle$, λ_{12} is the corresponding reorganization energy [5] and V_{jn} is the electronic coupling between states $|j\rangle$ and $|n\rangle$. The other possible mechanism involves a sequential process whereby the electron transfers from level $|1\rangle$ to $|2\rangle$ and then from $|2\rangle$ to $|3\rangle$. This mechanism is described by rates K_{21} and K_{32} and does not involve K_{31}. In the superexchange mechanism level $|2\rangle$ is never populated and the electron tunnels from level $|1\rangle$ to $|3\rangle$. Level $|2\rangle$ simply contributes to the tunneling matrix element (eq. (2)). Another way of stating this is that due to the energy-time uncertainty relation, the system can spend only a very short time $\approx\hbar/(\Delta G^0_{12} - \lambda_{12})$ in that level. Consequently, the dynamics of level $|2\rangle$ does not affect the rate. All we need to know is its thermally averaged energy. In the sequential mech-

[1] Camille and Henry Dreyfus Teacher/Scholar.

anism on the other hand, level $|2\rangle$ is intermediate in the kinetic scheme $|1\rangle \rightarrow |2\rangle \rightarrow |3\rangle$ and it could be populated during the course of the reaction. Ultrafast optical measurements [6] have shown that the rate of appearance of level $|3\rangle$ following the preparation of level $|1\rangle$ by photoexcitation is 3.6×10^{11} s^{-1}. These measurements have failed to detect a transient population of level $|2\rangle$. This observation could support the superexchange mechanism. However, a sequential scheme with $K_{32}/K_{21} \geqslant 70$ is also consistent with this result [7]. Extensive additional linear and nonlinear spectroscopic information (such as hole-burning and photon echo) is available for this system [8,9]. A major obstacle in resolving this issue is the lack of precise information regarding many of the relevant energetic parameters [3,4,10]. In particular the vertical transition energy $\Delta G^0_{12}-\lambda_{12}$ is not known. It should be emphasized that eqs. (1) and (2) hold only when $\Delta G^0_{12}-\lambda_{12}$ is large enough. V_{SE} diverges when $\Delta G^0_{12}-\lambda_{12}$ vanishes. In this paper we report a microscopic determination of K_{31} obtained by formulating the problem using the density matrix in Liouville space. This formulation was applied previously to nonadiabatic and adiabatic electron transfer in a two-level system and has been used to explore the role of the dynamics of solvation in electron transfer processes [11]. Our expression is valid for any value of $\Delta G^0_{12}-\lambda_{12}$ and can therefore be used to explore the interplay between superexchange and sequential electron transfer even when all three levels are degenerate.

2. Superexchange in a polar medium

We start our analysis by introducing the adiabatic (Born–Oppenheimer) model Hamiltonian for the system

$$H=\sum_{j=1}^{3}|j\rangle H_j\langle j| + V_{12}(|1\rangle\langle 2| + |2\rangle\langle 1|) + V_{23}(|2\rangle\langle 3| + |3\rangle\langle 2|)\,. \tag{3}$$

Here $H_j(Q)$ denotes the adiabatic Hamiltonian of the polar medium. V_{jn} represents the electronic coupling between states $|n\rangle$ and $|j\rangle$. The direct coupling V_{13} between states $|1\rangle$ and $|3\rangle$ was neglected in eq. (3) due to the large (17 Å) distance between the P and H molecules in the reaction center. The nuclear Hamiltonian $H_j(Q)$ can be partitioned into the following three terms:

$$H_j(Q)=E_j+H_B+U_j\,, \tag{4}$$

where E_j represents the electronic energy of the unsolvated state $|j\rangle$ and H_B represents the Hamiltonian of the bath, i.e. the nuclei of the RC which form a polar medium. U_j denotes the interaction between the electronic system and the medium, which may be expressed in terms of the polarization of the bath $\boldsymbol{P}(\boldsymbol{r})$, and the electrostatic field $\boldsymbol{D}_j(\boldsymbol{r})$ produced by the charge distribution of the system in the $|j\rangle$ state, i.e.

$$U_j=-\int \mathrm{d}r\, \boldsymbol{D}_j(\boldsymbol{r})\cdot\boldsymbol{P}(\boldsymbol{r})\,. \tag{5}$$

It should be emphasized that U_j depends on a macroscopic number of polarization degrees of freedom $\boldsymbol{P}(\boldsymbol{r})$, which undergo complicated motions resulting from thermal fluctuations. The statistical properties of U_j contain all the relevant information for our problem. We shall model U_j as Gaussian random variables. This is a common assumption in electron transfer theories [5]. It has been recently verified by an extensive numerical simulation of outer sphere electron transfer in water [12]. Eqs. (3)–(5) constitute our basic model Hamiltonian for the RC and they can be used to evaluate the electron transfer rates. We shall now introduce the following equilibrium density matrices for the bath

$$\rho_j=\exp(-H_j/k_BT)/\mathrm{Tr}\exp(-H_j/k_BT),\quad j=\mathrm{B},1,2,3\,, \tag{6}$$

where Tr denotes a trace over the bath degrees of freedom. ρ_B is the density matrix of the bath in the absence of the electron transfer system. ρ_1, ρ_2 and ρ_3 are the density matrices of the bath when the electron transfer system is in states 1, 2 and 3, respectively.

For the sake of simplicity we assume that the energy fluctuation U_j of the $|j\rangle$ state is totally uncorrelated with the energy fluctuation U_n on any other state $|n\rangle$, i.e.

$$\mathrm{Tr}(U_jU_n\rho_B)=0,\quad j\neq n\,. \tag{7}$$

This is a reasonable assumption for electron transfer

in the RC, because the different electronic states represent configurations in which the electron resides on different parts of the RC, which have a different local environment, and their energy fluctuations are expected to be uncorrelated. The present calculation of the rate is based on formulating the dynamics in terms of the density matrix in Liouville space [11]. The formalism allows a perturbative expansion of the rate matrix K_{jn} in a power series in the nonadiabatic coupling V. This formalism was developed for electron transfer in a two-level system resulting in general expressions for K_{21} and K_{32}. In this Letter we focus on the calculation of K_{31}. The calculation is very similar to the calculation of two-photon processes (two-photon absorption or fluorescence and Raman spectroscopy) [11,13]. The lowest order in V_{jn} which contributes to K_{31} is fourth order. When the calculation is done in Liouville space we find that there are three Liouville space pathways which contribute to K_{31} in fourth order, i.e.

$$K_{31} = 2\,\mathrm{Re}(K_{31}^{\mathrm{I}} + K_{31}^{\mathrm{II}} + K_{31}^{\mathrm{III}})\,. \tag{8}$$

These pathways are represented diagrammatically in fig. 1. Path I represents the process in which the electron transfers from state $|1\rangle$ to state $|3\rangle$ without actually passing through state $|2\rangle$. This is therefore a tunneling process. Paths II and III represent the process in which the electron does go through state $|2\rangle$, but before it equilibriates with the bath at state $|2\rangle$, the electron transfers to state $|3\rangle$. Of course, there is another process contributing to the population of state $|3\rangle$, i.e. the electron moving to state $|2\rangle$, equilibriating with the bath, and then transferring to state $|3\rangle$. This process is the sequential transfer, which is described by the rates K_{21} and K_{32}. If the relaxation of the system (RC and environment) is rapid enough, the contribution to K_{31} from paths II and III in fig. 1 can be ignored, so the only quantity we need to consider is K_{31}^{I}. This term can be evaluated using the static approximation for solvent fluctuations and assuming Gaussian statistics for U_j. The details of these calculations will be given elsewhere. Here we only present the final results for K_{31} in the high temperature limit. K_{31} is given in terms of several physical quantities (fig. 2). We first define the free energy change for the $|j\rangle$ to $|n\rangle$ transition

$$\Delta G_{jn}^{0} \equiv \mathrm{Tr}(H_j \rho_j) - \mathrm{Tr}(H_n \rho_n) \tag{9a}$$

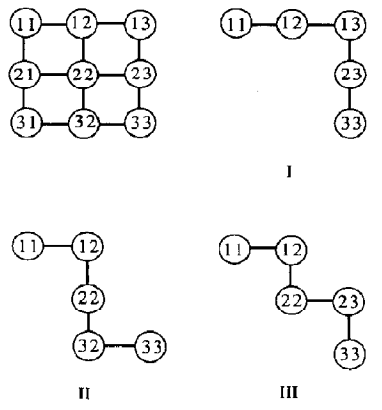

Fig. 1. The three Liouville-space pathways [10] contributing to the rate K_{31} to fourth order in the nonadiabatic coupling. Each pair of indexes jn implies that the system is in the state $|j\rangle\langle n|$, where $j = n$ stands for a population and $j \neq n$ for a coherence. Each bond represents a nonadiabatic coupling V. There are six pathways which can lead from 11 (upper left corner) to 33 (lower right) in fourth order (four bonds). These pathways come in complex conjugate pairs so that we need consider only the three pathways shown I, II and III. Pathway I which does not pass through a population in level 2 (eq. (22)) represents the tunneling (superexchange) mechanism and was evaluated explicitly in the present theory. Pathways II and III represent a sequential noncquilibrium process whereby the system goes through level 2 and proceeds to state 3 before thermal equilibrium. The contribution of these pathways may be made arbitrarily small if the medium relaxation times are sufficiently rapid. These pathways were neglected in the present theory.

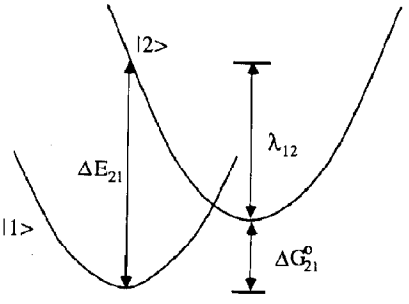

Fig. 2. Configuration coordinate scheme showing the transition free energy ΔG_{21}^{0}, the reorganization energy λ_{12} and the vertical transition energy ΔE_{21}. Similar schemes apply for the other pairs of levels (13 and 23).

and the vertical transition energy for this transition when the system is in state $|1\rangle$

$$\Delta E_{jn} \equiv \mathrm{Tr}[(H_j - H_n)\rho_1] . \tag{9b}$$

We further define the solvent reorganization energy in the $|j\rangle$ state,

$$\lambda_j \equiv \mathrm{Tr}(U_j^2 \rho_B)/2k_B T \tag{10}$$

and the reorganization energy for the $|j\rangle$ to $|n\rangle$ transition,

$$\lambda_{jn} \equiv \lambda_j + \lambda_n . \tag{11}$$

Using our Liouville space coupling scheme [11] we get

$$K_{31} = \frac{2V_{12}^2 V_{23}^2}{\hbar} \mathrm{Re} \int_0^\infty \mathrm{d}t_1 \int_0^\infty \mathrm{d}t_2 \int_0^\infty \mathrm{d}t_3 \times \exp(-\mathrm{i}\,\Delta E_{23} t_1 - \mathrm{i}\,\Delta E_{13} t_2 - \mathrm{i}\,\Delta E_{12} t_3) \times \exp\{-k_B T[\lambda_1 (t_2 + t_3)^2 + \lambda_2 (t_1 - t_3)^2 + \lambda_3 (t_1 + t_2)^2]\} . \tag{12}$$

When the time integrations in eq. (12) are carried out, the superexchange rate is finally given by

$$K_{31} = \frac{2\pi}{\hbar} V_{12}^2 V_{23}^2 [R_{13} I(\eta_{13})\, S_{13}(\Delta E_{13}) - R_{12} I(\eta_{12})\, S_{12}(\Delta E_{12}) - R_{23} I(\eta_{23})\, S_{23}(\Delta E_{23})] . \tag{13}$$

Here

$$R_{jk} = \frac{\lambda_{jk}}{(\lambda_1\lambda_2 + \lambda_1\lambda_3 + \lambda_2\lambda_3) 2k_B T} , \tag{14a}$$

$$\eta_{jn} = \sqrt{R_{jn}}\, \frac{\Delta E_{jm}\lambda_n + \Delta E_{nm}\lambda_j}{\lambda_{jn}} , \tag{14b}$$

$$S_{jn}(x) = \frac{1}{\sqrt{4\pi k_B T \lambda_{jn}}} \exp\left(- \frac{x^2}{4k_B T \lambda_{jn}} \right) , \tag{14c}$$

where j, n, m are permutations of 1, 2, 3. $S_{jn}(x)$ is just a Franck–Condon-weighted density of states. Using the definitions (9)–(11) we have

$$\Delta E_{12} = \Delta G_{12}^0 - \lambda_{12} , \tag{15a}$$

$$\Delta E_{13} = \Delta G_{13}^0 - \lambda_{13} , \tag{15b}$$

$$\Delta E_{23} = \Delta G_{23}^0 + \lambda_2 - \lambda_3 . \tag{15c}$$

Note that $\Delta E_{jn} = -\Delta E_{nj}$, $\Delta G_{jn}^0 = -\Delta G_{nj}^0$ and $\lambda_{jn} = \lambda_{nj}$.

The function $I(x)$ is given by

$$I(x) = -\int_0^\infty t \cos(xt) \exp(-t^2/2)\,\mathrm{d}t . \tag{16}$$

We have constructed the following Padé approximant, which provides a very good fit (better than 4%) for $I(x)$:

$$I(x) \approx \frac{-1 + 0.5851x^2}{1 + 0.4149x^2 + 0.1235x^4} , \quad |x| < 2.1 , \qquad \approx \frac{-1 + 0.5994x^2}{11.2551 - 3.8396x^2 + 0.5994x^4} , \quad |x| \geqslant 2.1 . \tag{17a}$$

Note the following limiting behavior of $I(x)$:

$$I(x) = \frac{1}{x^2} , \quad x \gg 1 , \qquad = -1 + \tfrac{1}{2}x^2 , \quad x \ll 1 . \tag{17b}$$

The general expression of the reverse rate K_{13} can be obtained from (13) and (14) by replacing the vertical transition energies ΔE_{13}, ΔE_{23} and ΔE_{12} by $\Delta G_{13}^0 + \lambda_{13}$, $\Delta G_{23}^0 + \lambda_{23}$ and $\Delta G_{12}^0 + \lambda_1 - \lambda_2$, respectively. Eqs. (13) and (14) which hold for any value of the energy parameters are the main result of this paper. The fluctuations in the energy levels $|1\rangle$, $|2\rangle$ and $|3\rangle$ are fully incorporated in this theory and this is why it holds for arbitrary values of ΔG_{jn}^0 and λ_{jn}. In contrast, the simple superexchange matrix element (eq. (2)) depends only on the average over the fluctuations and consequently it breaks down when $\Delta G_{12}^0 - \lambda_{12}$ vanishes. It should be noted that for certain values of the parameters, K_{31} (eq. (13)) can become negative. This may happen when $\Delta E_{13} \gg \sqrt{k_B T \lambda_{13}}$ and level E_2 is located between E_1 and E_3. In this case the system cannot be described by simple rate equations and one should calculate the frequency-dependent rate $K_{31}(s)$ which enters in a generalized rate equation (with a memory) [11]. Our K_{31} is then equal to the zero frequency value of the generalized rate $K_{31}(s=0)$. For the subsequent discussion we recall that the nonadiabatic rates K_{21}

and K_{32} are given within the same approximation by [5]

$$K_{21} = \frac{2\pi}{\hbar} |V_{12}|^2 S_{12}(\Delta G^0_{12} - \lambda_{12}) , \quad (18a)$$

$$K_{32} = \frac{2\pi}{\hbar} |V_{23}|^2 S_{23}(\Delta G^0_{23} - \lambda_{23}) . \quad (18b)$$

We shall now examine a few limiting cases of eq. (13). We first consider the case where the energy level $|2\rangle$ is sufficiently far from the energy levels $|1\rangle$ and $|3\rangle$, i.e.

$$\Delta E_{12} \gg \sqrt{\lambda_{12} k_B T}, \quad \Delta E_{23} \gg \sqrt{\lambda_{23} k_B T} . \quad (19)$$

Condition (19) implies that the activation energies $\Delta G^*_{12} \equiv (\Delta G^0_{12} - \lambda_{12})^2/4\lambda_{12}$ and $\Delta G^*_{23} \equiv (\Delta G^0_{23} + \lambda_2 - \lambda_3)^2/4\lambda_{23}$ are much larger than $k_B T$. This limit is where the conventional superexchange theory is usually formulated [3,4,14,15]. In this case eq. (13) assumes the form

$$K_{31} = \frac{2\pi}{\hbar} |V_{SE}|^2 S_{13}(\Delta E_{13}) , \quad (20a)$$

with

$$V_{SE} = \frac{V_{12} V_{23}}{\Delta E_{12}(\lambda_3/\lambda_{13}) + \Delta E_{32}(\lambda_1/\lambda_{13})} . \quad (20b)$$

Eqs. (20) reduce to the ordinary superexchange rate (1) and (2) when the electron transfer process is activationless, i.e. $\Delta E_{13} = 0$, so that $\Delta E_{12} = \Delta E_{32}$. In this limit K_{31} and the reverse rate K_{13} satisfy the detailed-balance condition

$$\frac{K_{13}}{K_{31}} = \exp\left(-\frac{\Delta G^0_{13}}{k_B T}\right) . \quad (21)$$

We next consider another limiting case where all three states are completely degenerate, i.e. $\Delta E_{12} = \Delta E_{23} = \Delta E_{13} = 0$. We further assume $\lambda_1 = \lambda_2 = \lambda_3 \equiv \lambda$. We then obtain from eq. (13)

$$K_{31} = \frac{2\pi}{\hbar} |V_{SE}|^2 S_{13}(0) , \quad (22a)$$

where

$$V_{SE} = \frac{V_{12} V_{23}}{\sqrt{3\lambda k_B T}} . \quad (22b)$$

Eqs. (22) may be rationalized using a simple physical argument. The variance of the energy level fluctuations is $\approx \sqrt{\lambda k_B T}$. V_{SE} is thus given by $V_{12} V_{23}$ divided by a typical energy fluctuation.

3. Application to the photosynthetic reaction center

We have calculated K_{31} using eq. (13) and the results are displayed as a function of $\Delta E_{21} = \Delta G^0_{21} + \lambda_{12}$ for different activation energies ΔE_{13} (fig. 3a)

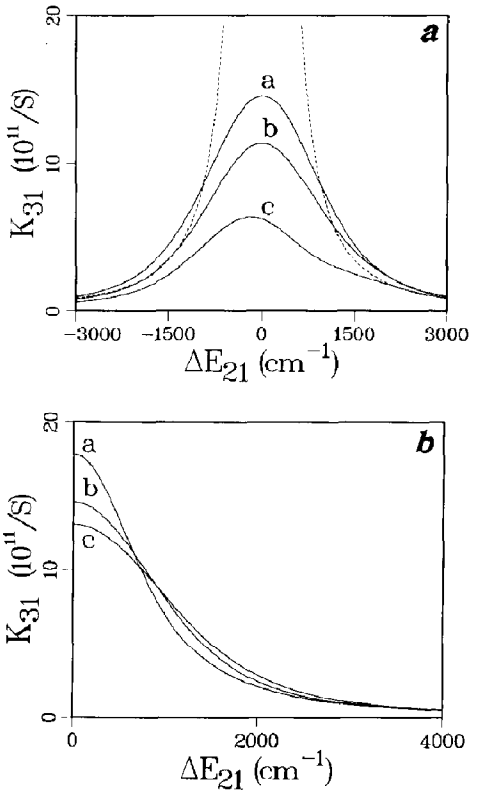

Fig. 3 (a) The dependence of the superexchange rate K_{31} on ΔE_{21} for different values of ΔE_{13}. Curves a, b and c correspond to $\Delta E_{13} = 0$, 400 and 700 cm^{-1}, respectively. The other parameters in this calculation are: $\lambda_{12} = 1000$ cm^{-1}, $\lambda_{23} = 1500$ cm^{-1}, $\lambda_{13} = 2000$ cm^{-1}, $V_{12} = 80$ cm^{-1}, $V_{23} = 6V_{12}$, $T = 300$ K. The dashed line represents the conventional superexchange rate (eqs. (20)) with $\Delta E_{13} = 0$. (b) The superexchange rate K_{31} versus ΔE_{21} for different values of the reorganization energy λ_{12}. Curves a, b and c correspond to $\lambda_{12} = 500$, 1000 and 2500 cm^{-1}, respectively. The other parameters are $\Delta E_{13} = 0$, $\lambda_{13} = 2000$ cm^{-1}, $V_{12} = 80$ cm^{-1}, $V_{23} = 6V_{12}$, $T = 300$ K.

and reorganization energies λ_{12} (fig. 3b). The dashed line in fig. 4 represents the asymptotic rate expression (eqs. (20)). Fig. 3 also demonstrates that ΔE_{13} and λ_{12} have a strong effect on the rate K_{31} for small values of ΔE_{21} and have a negligible effect for large values of ΔE_{21}, where the asymptotic rate expression (eqs. (20)) holds. Assuming that $K_{32} \gg K_{21}$, as suggested by the ultrafast measurements [6,7], then the sequential rate is basically equal to K_{21}. The following dimensionless parameter,

$$R \equiv \frac{K_{31}}{K_{31}+K_{21}}, \tag{23}$$

provides a measure of the relative contribution of the superexchange and the sequential mechanisms. R is bounded between 0 and 1. $R \to 0$ when the sequential transfer dominates, and $R \to 1$ when the superexchange transfer dominates. Fig. 4a displays the dependence of R on the energy ΔE_{21} for different values of λ_{12}. Estimates of the various parameters in the RC vary considerably among authors [2]. In the following discussion we shall use the parameters $V_{23}/V_{12}=6$, $\Delta E_{13}=0$, $\lambda_{13}=2000\ \mathrm{cm}^{-1}$. We further recall that the rise rate of level $|1\rangle$ following the preparation of level $|1\rangle$ is $3.6\times10^{11}\ \mathrm{s}^{-1}$. If the superexchange mechanism is dominant this should be the value of K_{31}. We have varied ΔE_{21}, λ_{12}, λ_{23} and V_{12} and searched for ranges of parameters for which the superexchange mechanism is dominant, defined as $R \geq 0.9$. It is clear that in order to reproduce the experimental rise-time of level $|3\rangle$, V_{12} has to be larger than some minimum value $V_{12}^{\min}$ which depends on the other parameters. We found that λ_{23} has little effect on $V_{12}^{\min}$, changing it by less than 2 cm^{-1} as λ_{23} varies from 1500 to 3000 cm^{-1}. Fig. 4b displays $V_{12}^{\min}$ (solid line) plotted against λ_{12}. For each value of $V_{12}^{\min}$, the superexchange mechanism will be dominant if ΔE_{21} is large enough. We have defined $\Delta E_{21}^{\min}$ to be the value of ΔE_{21} for which $R=0.9$, for a given λ_{12} and $V_{12}^{\min}$. For $\Delta E_{21} \geq \Delta E_{21}^{\min}$ the superexchange mechanism is dominant. $\Delta E_{21}^{\min}$ is also displayed in fig. 4b (dashed line). We conclude from fig. 4b that in order for the superexchange mechanisms to be dominant, the coupling constant V_{12} must be larger than 73 cm^{-1}.

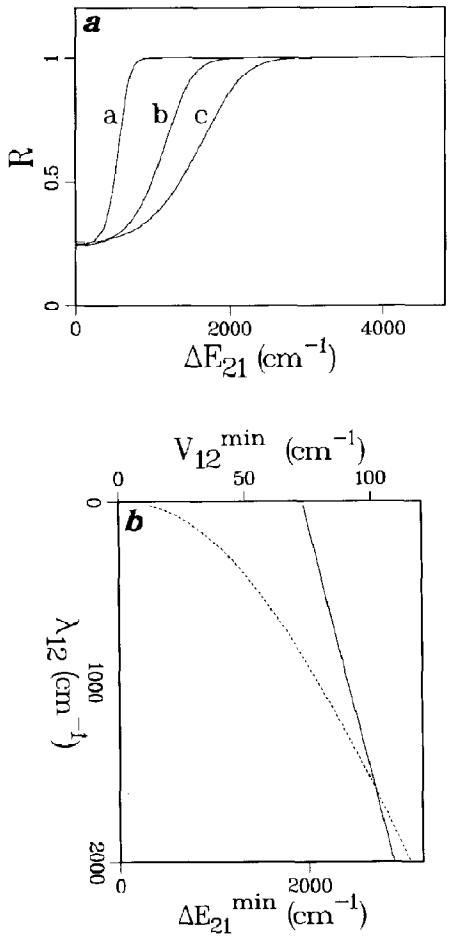

Fig. 4. (a) The relative contribution of the superexchange mechanism R versus ΔE_{21} for different values of the reorganization energy λ_{12}. Curves a, b and c correspond to $\lambda_{12}=100$, 500 and 1000 cm^{-1}, respectively. The other parameters are: $\lambda_{13}=2000$ cm^{-1}, $\lambda_{23}=2000\ \mathrm{cm}^{-1}$, $V_{12}=80\ \mathrm{cm}^{-1}$, $V_{23}=6V_{12}$, $T=300$ K. (b) The minimum coupling $V_{12}^{\min}$ (solid line) and the corresponding minimum energy $\Delta E_{21}^{\min}$ (dashed line) required for the superexchange mechanisms to be dominant ($R \geq 0.9$), are plotted versus λ_{12}. The other parameters are $\lambda_{13}=2000\ \mathrm{cm}^{-1}$, $\Delta E_{13}=0$, $V_{23}=6V_{12}$, $T=300$ K.

Our rate expression (eq. (13)) was obtained in the high temperature limit. In order to extend it to low temperatures we need to adopt a more specific model for H_B and U_j. A common model in electron transfer theories assumes that U_j is proportional to a simple harmonic coordinate representing an intramolecular or intermolecular vibration. In this case eqs. (13) should be modified by replacing all k_BT factors by the average oscillator energy $\langle \epsilon \rangle$ [7,16]

$$\langle \epsilon \rangle = \tfrac{1}{2}\hbar\omega \coth\left(\frac{\hbar\omega}{2k_B T}\right). \quad (24)$$

Note that in the high temperature ($k_B T \gg \hbar\omega$) limit $\langle \epsilon \rangle = k_B T$. When $k_B T$ in eq. (13) is replaced by $\langle \epsilon \rangle$ (eq. (24)) we obtain a rate expression which is not restricted to the high temperature limit. Martin et al. [7] have measured the temperature dependence of the RC electron transfer in the range 10 to 300 K. For *Rb. sphaeroides* the variation of the rate was found to be in agreement with the conventional superexchange rate assuming a single mode with $\omega = 80$ cm^{-1}. For *Rps. virides* on the other hand the conventional expression is inadequate and the best fit obtained [7] (using $\omega = 25$ cm^{-1}) is shown in fig. 5 (dashed line). Fig. 5 also shows the temperature dependence of our new expression for K_{31} (eq. (13) together with eq. (24)). It is clear that our expression is in better agreement with experiment than the ordinary superexchange rate.

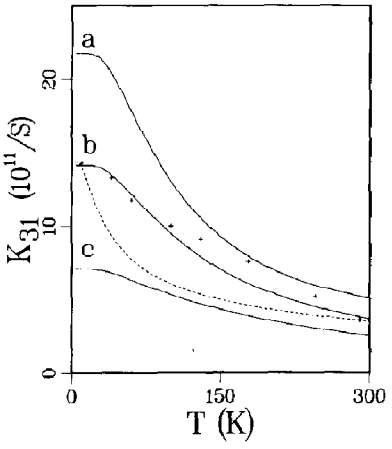

Fig. 5. Temperature dependence of the superexchange rate K_{31}. A coupling to a single vibrational mode with $\omega = 90$ cm^{-1} is assumed and the calculation used eq. (13) with $k_B T$ replaced by $\langle \epsilon \rangle$ (eq. (24)). Curves a, b and c correspond to $\Delta E_{21} = 800$ cm^{-1}, $\Delta E_{21} = 1050$ cm^{-1} and $\Delta E_{21} = 1500$ cm^{-1}, respectively. The dashed curve represents the best fit with the conventional superexchange rate using $\omega = 25$ cm^{-1} (eq. (2) in ref. [7]). The points (+) show the experimental electron transfer rate in *Rps. viridis* from Martin et al. [7]. Other parameters in this calculation are $\lambda_{13} = 2000$ cm^{-1}, $\lambda_{12} = 200$ cm^{-1}, $\lambda_{23} = 2000$ cm^{-1}, $V_{12} = 79$ cm^{-1}, $V_{23} = 6V_{12}$, $\Delta E_{13} = 0$. This figure shows that our superexchange expression (curve b) provides a better fit with experiment than the conventional superexchange expression (dashed curve).

Acknowledgement

The support of the Office of Naval Research, the National Science Foundation and the Petroleum Research Fund, administered by the American Chemical Society, is gratefully acknowledged.

References

[1] J. Deisenhofer, O. Epp, M. Miki, R. Huber and H. Michel, Nature 318 (1985) 618.
[2] J. Breton and A. Vermeglio, eds., The photosynthetic bacterial reaction center (Plenum Press, New York, 1988).
[3] R.A. Marcus, Chem. Phys. Letters 133 (1987) 471; in: The photosynthetic bacterial reaction center, eds. J. Breton and A. Vermeglio (Plenum Press, New York, 1988) p. 389.
[4] M. Bixon, J. Jortner, M. Plato and M.E. Michel-Beyerle, in: The photosynthetic bacterial reaction center, eds. J. Breton and A. Vermeglio (Plenum Press, New York, 1988) p. 399.
[5] R.A. Marcus and N. Sutin, Biochim. Biophys. Acta 811 (1985) 265.
[6] J. Breton, J.L. Martin, A. Migus, A. Antonetti and A. Orszag, Proc. Natl. Acad. Sci. US 83 (1986) 5121;
G.R. Fleming, J.L. Martin and J. Breton, Nature 333 (1988) 190.
[7] J.L. Martin, J. Breton, J.C. Lambry and G.R. Fleming, in: The photosynthetic bacterial reaction center, eds. J. Breton and A. Vermeglio (Plenum Press, New York, 1988) p. 195.
[8] J.M. Hayes and G.S. Small, J. Phys. Chem. 90 (1986) 4928;
S.R. Meech, A.J. Hoff and D.A. Wiersma, Chem. Phys. Letters 121 (1985) 287;
S.J. Boxer, D.S. Gottfried, D.J. Lockhart and T.R. Midderdorf, J. Chem. Phys. 86 (1987) 2439.
[9] Y. Won and R.A. Friesner, J. Phys. Chem. 92 (1988) 2214.
[10] Y. Won and R.A. Friesner, Biochim. Biophys. Acta 935 (1988) 9.
[11] M. Sparpaglione and S. Mukamel, J. Chem. Phys. 88 (1988) 5;
Y.J. Yan, M. Sparpaglione and S. Mukamel, J. Phys. Chem. 92 (1988) 4842.
[12] J.S. Bader and D. Chandler, Chem. Phys. Letters 157 (1989) 501.
[13] S. Mukamel, Advan. Chem. Phys. 70 (1988) 165.
[14] R. Hoffmann, A. Inamura and W. Hehne, J. Chem. Soc. (1968) 1499;
E. Stein and H. Taube, J. Am. Chem. Soc. 103 (1981) 693.
[15] A. Beretan and J.J. Hopfield, J. Am. Chem. Soc. 106 (1984) 1584;
M. Redi and J.J. Hopfield, J. Chem. Phys. 72 (1980) 6651;
J.R. Miller and J.V. Beitz, J. Chem. Phys. 74 (1981) 6746.
[16] M. Bixon and J. Jortner, J. Phys. Chem. 90 (1986) 3795.